Relation of arterial pressure waveform to left ventricular and carotid anatomy in normotensive subjects

JACC Vol. 22, No. 7
December 1993:1873–80

Relation of Arterial Pressure Waveform to Left Ventricular and Carotid Anatomy in Normotensive Subjects

PIER SERGIO SABA, MD,* MARY J. ROMAN, MD, FACC, RICCARDO PINI, MD,
MARIANE SPITZER, RDMS, ANTONELLO GANAU, MD,*
RICHARD B. DEVEREUX, MD, FACC
New York, New York and Sassari, Italy

Objectives. **The purpose of this study was to examine the relation of the central arterial pressure waveform to left ventricular and carotid structure.**

Background. **The pressure waveform in the central arteries is affected by reflection of the pressure wave from the periphery. When reflected waves merge with the incident wave during systole, a late systolic peak and increment in systolic blood pressure are observed. The consequent increase in hemodynamic load may stimulate left ventricular and vascular adaptive changes.**

Methods. **Sixty-seven normotensive adults were studied by noninvasive techniques. Anatomy and function of the left ventricle and carotid artery were investigated by ultrasonography. Pressure waveforms were recorded by an external tonometer applied to the carotid artery, and waveform shape was expressed by the augmentation index, calculated from the difference between the maximal systolic pressure and that at the inflection between early and late systolic pressure peaks divided by the pulse pressure. Subjects were assigned to groups with a dominant early (group 1, augmentation index ≤0) or dominant late systolic peak (group 2, augmentation index >0).**

Results. **Left ventricular mass index was significantly higher in group 2 than in group 1, a difference that persisted after controlling for the confounding effects of gender, age and blood pressure. Carotid wall thickness and regional arterial stiffness were significantly increased in group 2, but differences disappeared in the analysis of covariance for age.**

Conclusions. **Left ventricular and carotid artery structure are related to the shape of the central pressure waveform. Although the increase in left ventricular mass seen in subjects with a dominant late systolic peak pressure appears to be directly related to the shape of the pressure waveform, changes in the structural and physical properties of the carotid artery appear to be more closely related to the aging process.**

(J Am Coll Cardiol 1993;22:1873–80)

The arterial pressure waveform is the product of the interaction between the left ventricle and the vasculature. Blood ejected by the left ventricle generates a pressure wave that distends the wall of the aorta and subsequent arterial branches as it propagates along the arterial tree. Two components determine the shape of this wave: a forward wave that travels toward the periphery and a reflected wave that travels toward the heart (1,2). In the presence of optimal functional matching between the left ventricle and the vascular system, reflected waves fall in the diastolic portion of the central arterial waveform and generate a pressure increase that enhances coronary perfusion (3,4).

From the Department of Medicine, The New York Hospital–Cornell Medical Center, New York, New York and *Institute of Clinical Medicine, University of Sassari, Sassari, Italy. This study was supported in part by Grant HL 18323 from the National Heart, Lung, and Blood Institute, National Institutes of Health, Bethesda, Maryland; the Michael Wolk Heart Foundation, New York and the Helen W. Buckner Cardiac Research Fund, New York. Dr. Saba is the recipient of a research grant from the Regione Autonoma della Sardegna, Italy.

Manuscript received December 18, 1992; revised manuscript received May 7, 1993, accepted July 15, 1993.

Address for correspondence: Dr. Mary J. Roman, Division of Cardiology, Box 222, The New York Hospital–Cornell Medical Center, 525 East 68 Street, New York, New York 10021.

Alterations in vascular properties due to aging (5,6), hypertension (7,8), atherosclerosis (9,10) and high salt intake (7,11) lead to increased pulsed wave velocity and earlier return of reflected waves. Early reflected waves may reach the central circulation in late systole rather than diastole, further augmenting systolic pressure (2,3). The relevance of this phenomenon to left ventricular performance is suggested by evidence that early return of reflected waves (12) and a late systolic peak in the central pressure waveform (13–15) are associated with higher vascular impedance, an index of cardiac hydraulic load (16). Furthermore, an increase in systolic wall stress in the central arteries may induce structural adaptive changes of the vasculature.

Traditionally, high quality central pressure waveforms could be obtained only by invasive techniques. Thus, study of their configuration and significance has been limited to small numbers of subjects undergoing cardiac catheterization (12–16). The recent development of noninvasive devices that accurately record pressure waveforms in the carotid artery or other large arteries has led to evaluation in larger groups (17).

Nevertheless, there is a lack of information with regard to the influence of the arterial pressure waveform on left ventricular and arterial structure. The present study utilized

0735-1097/93/$6.00

JACC Vol. 22, No. 7
December 1993:1873–80

noninvasive, high fidelity recording of central pressure waveforms and ultrasound evaluation of carotid and left ventricular structure to examine these relations in normotensive, apparently normal, subjects.

Methods

Subjects. The study group comprised 67 normotensive adults (blood pressure <140/90 mm Hg on repeated measurements), with a mean age of 47 ± 15 years (range 26 to 85). Twenty-eight percent (19 subjects) were women, and 24% (16 subjects) were black. Fifty-one subjects (77%) had never smoked, 15 subjects (23%) were current or former smokers and information with regard to smoking history was unavailable in 1 subject. No subject had clinical evidence of coronary or cerebrovascular disease or diabetes mellitus, and none were taking medications. The presence of valvular heart disease was excluded by Doppler echocardiography. Body habitus was evaluated by body mass index, a measure of obesity (weight [kg] divided by height [m^2]) and body surface area. The study was conducted in accordance with protocols approved by the Committee on Human Rights in Research, Cornell University Medical College in 1989 and thereafter.

Echocardiography. A skilled research technician performed standard M-mode and two-dimensional echocardiograms in all subjects using a commercially available echocardiograph with 2.5- and 3.5-MHz imaging transducers. Left ventricular dimensions were obtained by averaging measurements made from two-dimensionally guided M-mode tracings according to recommendations of the American Society of Echocardiography (18) on up to six cycles with the use of a digitizing tablet. When M-mode tracings were technically inadequate, left ventricular dimensions were measured from the two-dimensional study using the method recommended by the American Society of Echocardiography (19). Left ventricular mass was calculated using the Penn convention (20) and adjusted for body surface area. Left ventricular geometry was further characterized by the relative wall thickness, calculated as follows: (2 × Posterior wall thickness)/End-diastolic dimension. Left ventricular end-systolic and end-diastolic volumes were calculated according to the Teichholz formula (21) to determine stroke volume. Total peripheral resistance and left ventricular fractional shortening were calculated using standard formulas. End-systolic meridional wall stress was calculated by the method of Reichek et al. (22). Carotid blood pressure at the dicrotic notch (aortic valve closure), derived from arterial pressure recording (see later), was used to estimate left ventricular end-systolic pressure.

Carotid ultrasonography. Carotid ultrasonography was performed using a Biosound Genesis II system (OTE Biomedica) equipped with a 7.5-MHz probe. With the subject supine and the neck in slight hyperextension, the common carotid artery, carotid bulb and extracranial portions of the internal and external carotid arteries were identified (23). Two-dimensionally guided M-mode tracings of the distal common carotid artery (approximately 1 cm proximal to the carotid bulb) with a simultaneous electrocardiogram and the pressure waveform from the contralateral carotid artery (described later) were recorded on 0.5-in. (1.27 cm) Super VHS videotape. Suitable frames for measurement of M-mode images were digitized using a frame-grabber (Imaging Technology, Inc.) interfaced with a high resolution (640 × 480 pixel) video monitor and stored on diskette. The axial resolution of the M-mode system is 0.2 mm at −6 dB.

Carotid measurements were performed on stored images using mouse-driven software written by one of us (Y.P.) after calibration for depth and time. The simultaneous carotid pressure tracing was used to time carotid artery measurement at end-diastole (minimal arterial pressure) and at the time of peak systolic pressure. Measurements included the combined intimal-medial thickness of the far wall at end-diastole, as has been validated in anatomic correlation studies (24,25), and end-diastolic and peak systolic internal dimensions obtained by continuous tracing of the intima-lumen interfaces of the near and far walls. All measurements were performed during several cycles and averaged. Arterial relative wall thickness at end-diastole was calculated as follows: (2 × Far-wall thickness)/Internal dimension.

Both carotid arteries were scanned to identify the presence and size of atherosclerotic plaques (25,26). Standard wall thickness measurements were never obtained at the level of a discrete plaque.

Carotid pressure waveforms. A high fidelity external pressure transducer (model SPT-301, Millar Instruments) applied to the skin overlying the pulse of a common carotid artery was used to obtain carotid pressure waveforms. Applanation of the curved surface of the artery, balancing circumferential stresses in its wall, allows accurate registration of pressure waveforms, as previously described by Drzewiecki et al. (27). Waveforms and modulus and phase of harmonic components obtained by using this external transducer closely resemble those derived from intraarterial recordings (28). The accuracy of the tonometer compared to simultaneous intraarterial recordings has been validated in the femoral artery in dogs (28) and the radial (28) and carotid (29–31) arteries in humans.

The transducer is internally calibrated (1 mV = 10 mm Hg) and registers absolute changes in blood pressure over a range of 300 mm Hg. To obtain actual carotid blood pressure values, the waveform tracings were also externally calibrated. On the basis of the observation that mean arterial pressure does not significantly vary within the capacitance vessels (32,33), brachial artery pressure was measured by cuff and mercury sphygmomanometer with the patient supine, and mean pressure was calculated as follows: Diastolic blood pressure + (1/3 × Pulse pressure). The obtained value was assigned to the planimetrically computer-derived mean blood pressure of the carotid waveforms. After calibration, carotid peak systolic and end-diastolic pressures were calculated by computer.

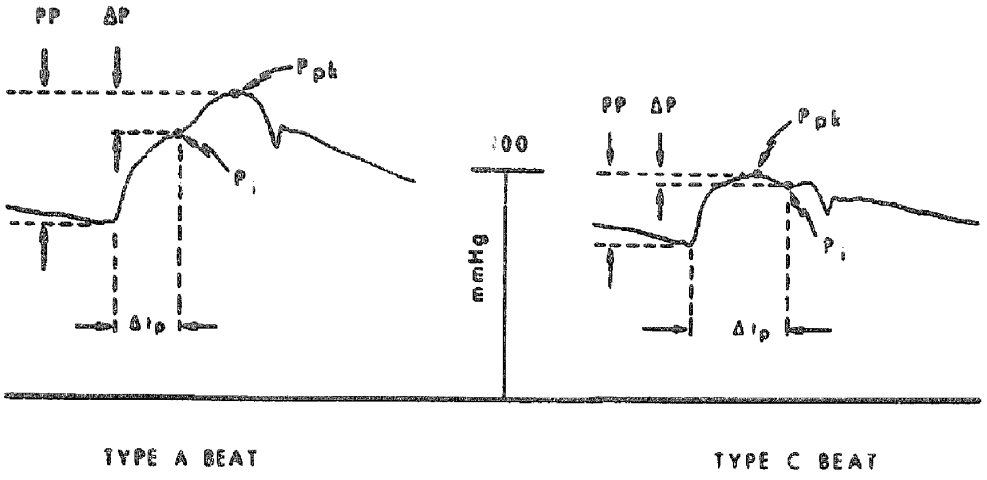

Figure 1. Calculation of the augmentation index (ratio $P_{pk} - P_i$)/(pulse pressure) from a central pressure recording in subjects with dominant late (type A beat) or early (type C beat) peak systolic pressure (see text). Reproduced from Murgo et al. (13), with permission of the American Heart Association, Inc. ΔP = the difference between peak systolic pressure and pressure at the inflection point; Δt_p = time to inflection point; P_i = inflection point; PP = pulse pressure; P_{pk} = peak systolic pressure.

The systolic portion of the carotid waveform was further analyzed to calculate the augmentation index (15,17,34), a means of quantifying the augmentation of systolic pressure due to the late systolic peak as a proportion of the pulse pressure. After identification of the early and late systolic peaks and the inflection that separates them, pressures were determined at peak systolic pressure (P_{pk}) and at the inflection point (P_i) using the previously described calibrated computer system. The augmentation index was calculated as ($P_{pk} - P_i$)/Pulse pressure, when P_{pk} occurred in late systole, or as ($P_i - P_{pk}$)/Pulse pressure, when P_{pk} occurred in early systole (13) (Fig. 1). Measurements were repeated during several cycles and averaged. Intraobserver reproducibility for this index was good ($r = 0.84$, SEE = 0.06, mean variation 6%) and was comparable to that of previous studies (34). On the basis of the configuration of the pressure waveform, subjects were classified according to the presence of type A, B, or C beats as classified by Murgo et al. (13): type A beat = augmentation index >0.12 (late systolic peak markedly higher than the early systolic peak); type B beat = augmentation index >0 but ≤0.12 (late systolic peak slightly higher than early systolic peak); type C beat = augmentation index ≤0 (early systolic peak equal to or higher than late systolic peak).

Arterial stiffness. Carotid artery stiffness was estimated by three methods (35). Peterson's elastic modulus (E_p) was calculated according to the following formula:

$$E_p = ([P_s - P_d]/[D_s - D_d]) \times D_d,$$

where P_s and P_d are systolic and diastolic pressures, respectively, and D_s and D_d are systolic and diastolic carotid diameters, respectively (36). Young's modulus (E) (wall tension per centimeter wall thickness for 100% diameter increase) was calculated according to the following formula:

$$E = ([P_s - P_d]/[D_s - D_d] \times (D/h),$$

where P_s, P_d, D_s and D_d are, as defined previously, the systolic and diastolic pressures and diameters, respectively, and D and h are the carotid mean diameter and wall thickness, respectively (37). Carotid stiffness was also calculated as β' (beta), according to the following formula (38,39):

$$\beta' = (\ln[P_s/P_d])/([D_s - D_d]/D_d),$$

which takes into account the curvilinear relation between arterial pressure and diameter. Because our system records simultaneous carotid images and pressure (Fig. 2), β was also determined at a standardized pressure of 100 mm Hg (β_{100}), according to the formula of Hirai et al. (35,39):

$$\beta_{100} = (\ln[P_s/P_d])/([D_s - D_d]/D_{100}),$$

where D_{100} is the carotid diameter at 100 mm Hg. This approach allows the influence of distending pressure on vascular stiffness to be standardized. Because of limitations of simultaneous pressure-dimension recordings, it was not possible to obtain β' in seven subjects and β_{100} in an additional five subjects whose range of arterial pressure did not include 100 mm Hg.

Statistical analysis. Data were analyzed using the Crunch[4] Statistical Package (Crunch Software Corporation) (40). Relations between continuous variables were evaluated by linear regression. Comparisons among more than two groups were performed by analysis of variance, followed by the Ryan, Einot, Gabriel and Welsch F test multiple comparison procedure, which is the most powerful of the tests based on the F distribution (40,41). Comparisons between subjects with an augmentation index ≤0 (group 1) and subjects with a positive augmentation index (>0) (group 2) were performed using the Student *t* test. Independent predictors of the augmentation index were determined using multiple regression analysis. To take into account the effect of gender, age and blood pressure, comparisons between the two groups of subjects were also performed by analysis of covariance. Mean values corrected for gender and age and for gender, age and mean blood pressure of subjects were calculated for each dependent variable. Data are expressed as mean value ± SD. A p value < 0.05 was considered significant.

JACC Vol. 22, No. 7
December 1993:1873–80

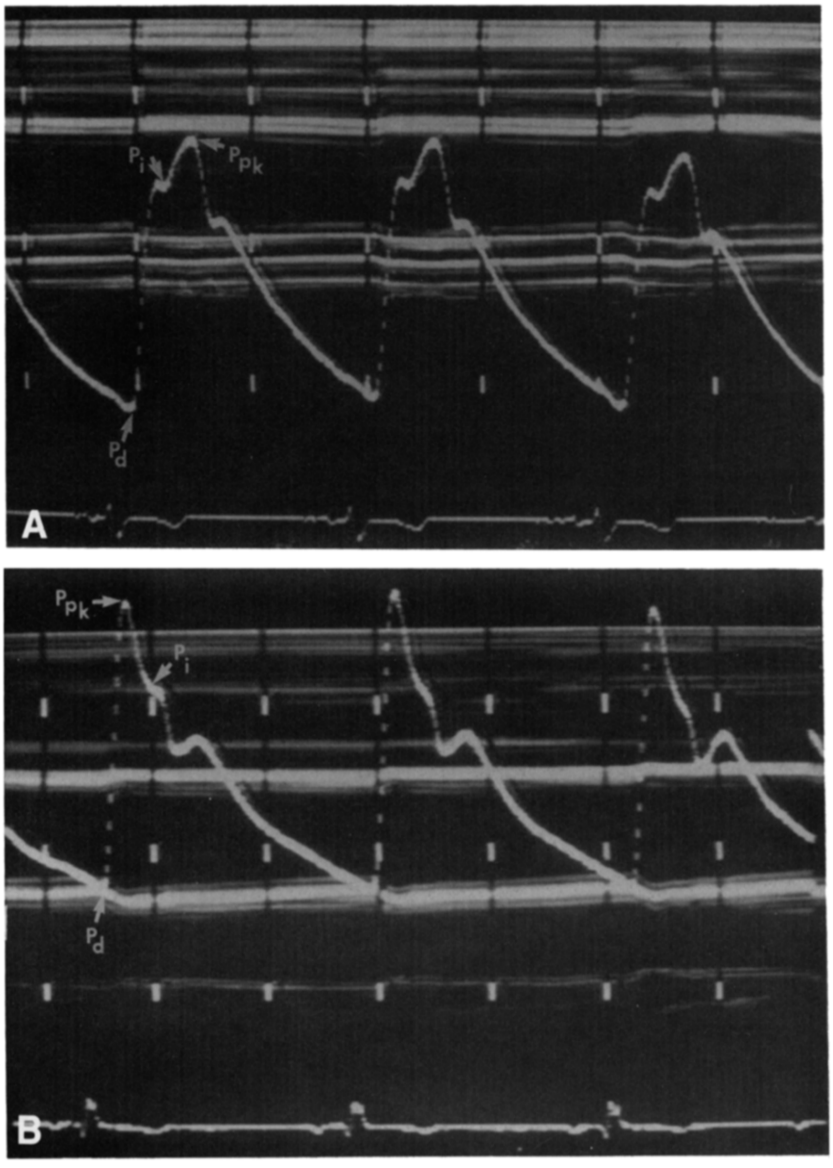

Figure 2. Examples of simultaneous M-mode tracing and pressure waveform of the common carotid artery in two subjects with a dominant late (A, type A beat in a 51-year old man) or early (B, type C beat in a 27 year-old man) peak systolic pressure and similar systolic blood pressure (118 and 120 mm Hg, respectively). P_d = diastolic pressure; other abbreviations as in Figure 1.

Results

Augmentation index and demographic variables. The 21 subjects with type A beats and the 21 subjects with type B beats were similar with regard to age, body size and blood pressure, although both groups were older and had a higher systolic and mean arterial blood pressure than did the 25 subjects with type C beats (Table 1). When the subjects with types A and B beats were combined (group 2) and compared with subjects with type C beats (group 1), the proportion of women was greater in group 2, and height was therefore lower (Table 2).

Carotid pulse pressure showed a tendency to be higher in group 2. As a consequence, the increase in pulse pressure between the carotid and brachial arteries, was less in subjects with a positive augmentation index (15% vs. 29%), although this difference did not reach statistical significance.

Augmentation index and left ventricular structure and function. Left ventricular wall thicknesses were greater in subjects with a dominant late systolic peak (group 2) than in those with a higher early systolic peak (group 1) (Table 3). Although left ventricular mass was not statistically different between the two groups, adjustment for body size identified larger indexed ventricular mass in group 2 (81 ± 18 vs. 69 ± 14 g/m^2, $p < 0.006$). After controlling for gender effects, left ventricular mass index was positively related ($r = 0.30$, $p < 0.02$) to the augmentation index (Fig. 3), whereas relations of ventricular mass to measures of arterial stiffness did not attain statistical significance. Because left ventricular end-diastolic chamber sizes were similar, relative wall thickness was higher in group 2. Total peripheral resistance was increased in group 2 subjects owing to the higher mean blood pressure because stroke volume and cardiac output did not differ statistically between the groups.

Augmentation index and carotid artery structure and stiffness. Carotid artery absolute and relative wall thicknesses were larger in group 2 than in group 1 (Table 4, Fig. 2). All measures of regional arterial stiffness (except Young's modulus, which did not attain statistical significance) were in-

Table 1. Augmentation Index Groups: Demographic Variables

	Type C Beat (AI ≤ 0.00) (n = 25)	Type B Beat (AI > 0.00 ≤ 0.12) (n = 21)	Type A Beat (AI > 0.12) (n = 21)
AI	−0.11 ± 0.08	0.07 ± 0.04	0.20 ± 0.07
Age (yr)	37 ± 11	51 ± 16*	55 ± 12*
Gender (M/F)	22/3	14/7	12/9
Height (m)	1.75 ± 0.08	1.68 ± 0.11†	1.69 ± 0.10†
Body mass index (kg/m²)	24.5 ± 4.5	25.4 ± 3.3	25.9 ± 4.1
Body surface area (m²)	1.91 ± 0.23	1.82 ± 0.23	1.84 ± 0.20
Brachial SBP (mm Hg)	116 ± 9	122 ± 12†	125 ± 8*
Brachial DBP (mm Hg)	68 ± 9	72 ± 11	75 ± 7†
Brachial PP (mm Hg)	48 ± 8	50 ± 10	49 ± 7
MAP (mm Hg)	84 ± 8	90 ± 10†	92 ± 7*
Carotid SBP (mm Hg)	107 ± 10	116 ± 14*	120 ± 9*
Carotid DBP (mm Hg)	67 ± 10	71 ± 14	72 ± 10
Carotid PP (mm Hg)	40 ± 12	46 ± 18	48 ± 13

*p < 0.05 vs. subjects with type C beat, †p < 0.01 vs. subjects with type C beat. Values presented are mean values ± SD or number of subjects. AI = augmentation index; DBP = diastolic blood pressure; F = female; M = male; MAP = mean arterial pressure; PP = pulse pressure; SBP = systolic blood pressure.

creased in group 2 subjects, even when the distending pressure was taken into account (β_{100}). The prevalence of atherosclerotic plaques was similar in groups 1 and 2 (4% and 14%, respectively).

Relation of age and blood pressure to augmentation index. In the study group as a whole, the augmentation index was most closely related to age (r = 0.52, p < 0.0001 (Fig. 4), similar to previous findings (17). The augmentation index was inversely related to height (r = −0.39, p < 0.01) but was not related to body mass index or body surface area. Both carotid (r = 0.35, p < 0.01) and brachial (r = 0.28, p < 0.05) systolic pressures and total peripheral resistance (r = 0.38, p < 0.01) were related to the augmentation index. In multiple regression analysis, independent predictors of the augmentation index included age (R^2 = 0.27, p < 0.0001), gender (R^2 = 0.09, p < 0.005) and mean arterial pressure (R^2 = 0.04, p < 0.05) but not height.

Analysis of covariance was performed to control for the impact of gender, age and blood pressure on the differences in left ventricular and carotid anatomy between the two groups (Tables 5 and 6). After adjustment for gender and

Table 2. Demographic Features and Arterial Pressures in Subjects With a Dominant Early or Late Systolic Peak of the Central Arterial Pressure Waveform

	Group 1 (type C beats, AI ≤ 0.0) (n = 25)	Group 2 (types A and B beats, AI > 0.0) (n = 42)	p Value
AI	−0.11 ± 0.08	0.14 ± 0.08	
Age (yr)	36 ± 10	54 ± 14	< 0.0001
Gender (M/F)	22/3	26/16	< 0.03
Smoking history (% smokers)	16	26	NS
Height (m)	1.76 ± 0.08	1.69 ± 0.10	< 0.002
Body mass index (kg/m²)	24.6 ± 4.5	25.6 ± 3.7	NS
Body surface area (m²)	1.92 ± 0.22	1.83 ± 0.21	NS
Brachial SBP (mm Hg)	116 ± 9	123 ± 10	< 0.005
Brachial DBP (mm Hg)	68 ± 9	74 ± 10	< 0.03
Brachial PP (mm Hg)	48 ± 8	50 ± 8	NS
MAP (mm Hg)	84 ± 8	90 ± 9	< 0.006
Carotid SBP (mm Hg)	107 ± 10	118 ± 12	< 0.0003
Carotid DBP (mm Hg)	67 ± 10	71 ± 12	NS
Carotid PP (mm Hg)	40 ± 12	47 ± 16	NS

Unless otherwise identified, values presented are mean value ± SD or number of subjects. Abbreviations as in Table 1.

Table 3. Relation of Augmentation Index to Left Ventricular Structure and Function

	Group 1 (AI ≤ 0.0) (n = 25)	Group 2 (AI > 0.0) (n = 42)	p Value
LV diastolic posterior wall thickness (cm)	0.7 ± 0.1	0.8 ± 0.1	< 0.004
IV septal diastolic thickness (cm)	0.8 ± 0.1	0.9 ± 0.1	< 0.02
LV diastolic internal diameter (cm)	5.0 ± 0.4	4.9 ± 0.5	NS
LV mass (g)	133 ± 35	149 ± 44	NS
LV mass index (g/m²)	69 ± 14	81 ± 18	< 0.006
Relative wall thickness	0.30 ± 0.05	0.34 ± 0.06	< 0.002
Total peripheral resistance (dynes·cm/s⁻⁵)	1,313 ± 269	1,630 ± 393	< 0.002
Stroke volume (ml)	78 ± 16	78 ± 17	NS
Cardiac output (liters/min)	5.3 ± 1.1	4.7 ± 1.3	NS
Fractional shortening (%)	36 ± 5	37 ± 5	NS
End-systolic stress (dynes/cm²·10³)*	57 ± 16	51 ± 11	NS

*Calculated using carotid dicrotic notch pressure. Values presented are mean value ± SD. AI = augmentation index; IV = interventricular; LV = left ventricular.

Figure 3. Relation of the residuals of the relation between left ventricular mass index and gender (vertical axis) and the augmentation index (horizontal axis). Gender adjustment is used because of the higher proportion of women among subjects with a higher augmentation index.

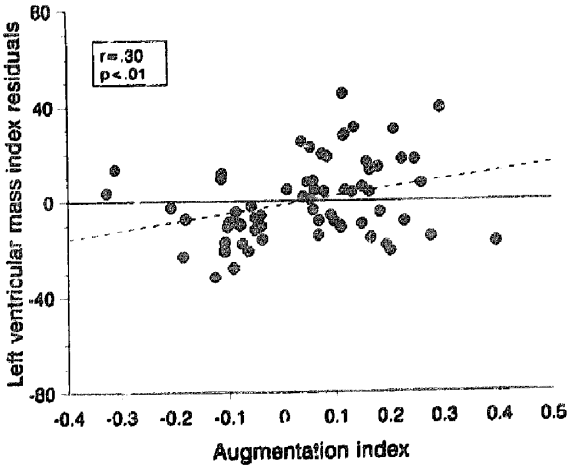

JACC Vol. 22, No. 7
December 1993:1873–80

Table 4. Relation of Augmentation Index to Carotid Artery Anatomy and Stiffness

	Group 1 (AI ≤ 0.0) (n = 25)	Group 2 (AI > 0.0) (n = 42)	p Value
Wall thickness (mm)	0.62 ± 0.17	0.73 ± 0.15	< 0.01
Diastolic dimension (mm)	5.77 ± 0.71	5.50 ± 0.60	NS
Relative wall thickness	0.22 ± 0.05	0.27 ± 0.06	< 0.0006
E_p (dynes/cm^2·10^{-6})	0.37 ± 0.18	0.53 ± 0.31	< 0.01
E (dynes/cm^2 per mm·10^{-6})	0.63 ± 0.19	0.75 ± 0.37	NS
β' (n = 60)	3.84 ± 1.92	5.66 ± 2.82	< 0.01
β_{100} (n = 55)	4.28 ± 2.16	6.03 ± 2.89	< 0.03

Values presented are mean value ± SD. AI = augmentation index; β' = beta (carotid stiffness index); β_{100} = beta at 100 mm Hg; E = Young's modulus; E_p = elastic modulus.

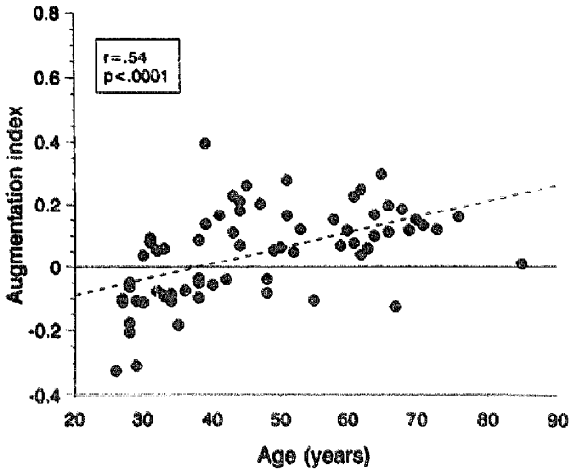

Figure 4. Relation of augmentation index to age in the study group.

age, left ventricular posterior wall and interventricular septal thicknesses remained higher in group 2 subjects (0.84 vs. 0.75 cm, $p < 0.01$, and 0.88 vs. 0.78 cm, $p < 0.05$, respectively), as did left ventricular mass index (83 vs. 65 g/m^2, $p < 0.001$). Conversely, previously detected differences in carotid artery structure and vascular stiffness were no longer significant. Further analysis with gender, age and mean arterial pressure as covariates confirmed significant differences in left ventricular wall thicknesses and mass index between the two groups (Table 5).

Discussion

Augmentation index and left ventricular structure. The present study examines the relation of the shape of the arterial pressure waveform to cardiac and vascular structure in apparently normal adults. Although age-related changes in the central waveform have been previously demonstrated (17,42–44), their impact on ventricular-vascular coupling has only been assessed by invasive methods in small, select patient groups (15). In the present study, application of noninvasive methods in normotensive subjects has revealed positive relations between the shape of the arterial pressure waveform in systole and several measures of vascular and cardiac structure and function. Most notably, higher indexed left ventricular mass was detected in subjects with late systolic augmentation of arterial pressure. Although women predominated in the group with a dominant late systolic peak with a consequent lower height and lesser distance between the central circulation and the sites of pressure wave reflection, this increase in ventricular mass became statistically more significant after adjustment for age, gender and blood pressure. A relation of augmentation index to height has recently been observed (31,45), although its impact on left ventricular mass was not examined in these studies.

The physiologic basis for the observed relation between the arterial pressure waveform and left ventricular structure may reflect the impact of arterial pressure on ventricular wall stress. Delay of peak systolic pressure into late systole will slow the normally rapid decline of ventricular wall stress after the peak level is reached in early systole (46) and thereby increase the integral of systolic left ventricular wall

Table 5. Left Ventricular Anatomy in Relation to Augmentation Index After Correction for Gender, Age and Mean Arterial Pressure by Analysis of Covariance

	Adjusted Mean Values* for Group 1 (n = 25) (AI ≤ 0.0)		Adjusted Mean Values* for Group 2 (n = 42) (AI > 0.0)	
	Age	Age + MAP	Age	Age + MAP
Height (m)	1.71	1.72	1.71	1.70
LV diastolic posterior wall thickness (cm)	0.75	0.76	0.84†	0.83‡
IV septal diastolic thickness (cm)	0.78	0.80	0.88§	0.87‡
LV mass index (g/m^2)	65	65	83‖	83¶
LV relative wall thickness	0.31	0.32	0.33	0.33
Total peripheral resistance (dynes·cm/s^{-5})	1,434	1,454	1,561	1,551

*Mean values are corrected for gender and age and for gender, age and mean arterial pressure of subjects, respectively. †$p < 0.01$ versus group 1 after adjustment for gender and age. ‡$p < 0.05$ versus group 1 after adjustment for gender, age and mean arterial pressure. §$p < 0.05$ versus group 1 after adjustment for gender and age. ‖$p < 0.001$ versus group 1 after adjustment for gender and age. ¶$p < 0.001$ versus group 1 after adjustment for gender, age and mean arterial pressure. Abbreviations as in Tables 1 and 3.

Table 6. Carotid Artery Structure and Stiffness in Relation to Augmentation Index After Correction for Gender, Age and Mean Arterial Pressure by Analysis of Covariance

	Adjusted Mean Values* for Group 1 (n = 25) (AI ≤ 0.0)		Adjusted Mean Values* for Group 2 (n = 42) (AI > 0.0)	
	Age	Age + MAP	Age	Age + MAP
Carotid SBP (mm Hg)	110	113	116	115
Carotid DBP (mm Hg)	66	70	72	69
Carotid wall thickness (mm)	0.68	0.70	0.69	0.69
Carotid relative wall thickness	0.24	0.24	0.26	0.25
E_p (dynes·cm^2·10^{-6})	0.48	0.48	0.47	0.47
E (dynes·cm^2/mm·10^{-6})	0.69	0.69	0.72	0.72
β' (n = 60)	5.02	4.95	4.92	4.97
β_{100} (n = 55)	5.66	5.51	5.31	5.38

*Mean values are corrected for gender and age and for gender, age and mean arterial pressure of subjects, respectively. Abbreviations as in Tables 1 and 4.

stress despite normal peak systolic and end-diastolic blood pressures. An increase in integrated left ventricular wall stress would in turn increase myocardial oxygen demand (47) and left ventricular mass because the tension imposed on cardiac myocytes is the single most important stimulus to myocardial cell growth (48,49). The association between late systolic pressure peaks and left ventricular relative wall thickness did not remain statistically significant after adjustment for gender and age.

Prospective evaluation will be required to determine whether subjects with a dominant late systolic arterial pressure waveform peak are more likely to develop frank left ventricular hypertrophy or isolated systolic hypertension, or both, than are those with a dominant early systolic peak. The observation that the pulsatile component of blood pressure is an independent risk factor for cardiovascular death (50) and is related to left ventricular hypertrophy (51,52) suggests that left ventricular hypertrophy may develop later in a disproportionate number of these subjects.

Augmentation index and carotid artery structure and function. The structure of the central conduit arteries, exemplified by the common carotid artery, was also found in the current study to be related to the pressure waveform. Similar to left ventricular findings, both the absolute and relative wall thicknesses of the common carotid artery were increased in subjects with a dominant late systolic pressure peak, whereas the internal diameters were similar in the two groups. All measures of regional arterial stiffness were increased in group 2 subjects, including measures that take into account the curvilinear pressure-volume relation (β' and β_{100}), the influences of distending pressure (β_{100}) or the effect of compensatory increases in wall thickness (Young's modulus).

The observed differences in carotid artery structure and stiffness between the two groups appear to be primarily related to differences in age based on the analyses of covariance. The present results confirm previous reports of a strong relation between age and the augmentation index (13,17,44). Development of late systolic peaks of the pressure waveform may therefore primarily reflect changes in arterial structure associated with the aging process (5,6,53). The potential contribution of atherosclerosis to these vascular changes could not be evaluated in the current study group with a low prevalence of atherosclerotic plaques (10%).

Conclusions. Left ventricular and carotid artery structure in normotensive adults are related to the shape of the central arterial pressure waveform. Although the increase in left ventricular mass seen in subjects with a dominant late systolic peak appears to be directly related to alterations in the shape of the pressure waveform independent of mean arterial pressure and age, changes in the structural and physical properties of the carotid artery could not be dissociated statistically from the aging process. In fact, it is possible, perhaps even likely, that the known effects of increasing age on the central arterial pressure waveform (17) are biologically mediated by thickening and increased stiffness of the capacitance vessels. Further studies are required to determine whether this is true and to clarify the independent prognostic significance, if any, of a dominant late systolic peak of the pressure waveform.

We thank Virginia Burns for assistance in preparation of the manuscript.

References

1. Remington JW, Wood EH. Formation of peripheral pulse contour in man. J Appl Physiol 1956;9:433–42.
2. Westerhof N, Sipkema P, Van Den Bos GC, Elzinga G. Forward and backward waves in the arterial system. Cardiovasc Res 1972;6:648–56.
3. O'Rourke MF, Yaginuma T. Wave reflection and the arterial pulse. Arch Intern Med 1984;144:366–71.
4. O'Rourke MF. Vascular impedance in studies of arterial and cardiac function. Physiol Rev 1982;62:570–623.
5. Hallock P. Arterial elasticity in man in relation to age as evaluated by the pulse wave velocity method. Arch Int Med 1934;54:770–98.
6. Avolio AP, Chen SG, Wang RP, Zhang CL, Li MF, O'Rourke MF. Effects of aging on changing arterial compliance and left ventricular load in a northern Chinese urban community. Circulation 1983;68:50–8.
7. Avolio AP, Deng FQ, Li WQ, et al. Effects of aging on arterial distensibility in populations with high and low prevalence of hypertension: comparison between urban and rural communities in China. Circulation 1985;71:202–10.
8. Ting CT, Brin KP, Lin SJ, et al. Arterial hemodynamics in human hypertension. J Clin Invest 1986;78:1462–71.
9. Farrar DJ, Green HD, Bond MG, Wagner WD, Gobbeé RA. Aortic pulse wave velocity, elasticity, and composition in a nonhuman primate model of atherosclerosis. Circ Res 1978;43:52–62.
10. Farrar DJ, Green HD, Wagner WD, Bond MG. Reduction in pulse wave velocity and improvement of aortic distensibility accompanying regression of atherosclerosis in the rhesus monkey. Circ Res 1980;47:425–32.
11. Avolio AP, Clyde KM, Beard TC, Cooke HM, Ho KKL, O'Rourke MF. Improved arterial distensibility in normotensive subjects on a low salt diet. Arteriosclerosis 1986;6:166–9.
12. Mills CJ, Gabe IT, Gault JH, et al. Pressure-flow relationships and vascular impedance in man. Cardiovasc Res 1970;4:405–17.
13. Murgo JP, Westerhof N, Giolma JP, Altobelli SA. Aortic input impedance

in normal man: relationship to pressure wave forms. Circulation 1980;62: 105–16.
14. Murgo JP, Westerhof N, Giolma JP, Altobelli SA. Manipulation of ascending aortic pressure and flow wave reflections with the Valsalva maneuver: relationship to input impedance. Circulation 1981;63:122–32.
15. Nichols WW, O'Rourke MF, Avolio AP, et al. Effects of age on ventricular-vascular coupling. Am J Cardiol 1985;55:1179–84.
16. O'Rourke MF, Taylor MG. Input impedance of the systemic circulation. Circ Res 1967;20:365–80.
17. Kelly R, Hayward C, Avolio A, O'Rourke M. Noninvasive determination of age-related changes in the human arterial pulse. Circulation 1989;80: 1652–9.
18. Sahn DJ, DeMaria A, Kisslo J, Weyman A. Recommendation regarding quantitation in M-mode echocardiography: results of a survey of echocardiographic measurements. Circulation 1978;58:1072–83.
19. Schiller NB, Shah PM, Crawford M, et al. Recommendation for quantitation of the left ventricle by two-dimensional echocardiography. J Am Soc Echocardiogr 1989;2:358–67.
20. Devereux RB, Reichek N. Echocardiographic determination of left ventricular mass in man: anatomic validation of the method. Circulation 1977;55:613–8.
21. Teichholz LE, Kreulen T, Herman MV, Gorlin R. Problems in echocardiographic volume determinations: echocardiographic-angiographic correlations in the presence or absence of asynergy. Am J Cardiol 1976;37: 7–11.
22. Reichek N, Wilson J, St John Sutton M, Plappert TA, Goldberg S, Hirschfeld JW. Non invasive determination of end-systolic stress: validation of the method and initial application. Circulation 1982;65:99–108.
23. Roman MJ, Saba PS, Pini R, et al. Parallel cardiac and vascular adaptation in hypertension. Circulation 1992;86:1909–18.
24. Pignoli P, Tremoli E, Poli A, Oreste P, Paoletti R. Intimal plus medial thickness of the arterial wall: a direct measurement with ultrasound imaging. Circulation 1986;74:1399–406.
25. Handa N, Matsumoto M, Maeda H, et al. Ultrasonic evaluation of early carotid atherosclerosis. Stroke 1990;21:1567–72.
26. Ricotta JJ, Bryan FA, Bond MG, et al. Multicenter validation study of real-time (B-mode) ultrasound, arteriography, and pathologic examination. J Vasc Surg 1987;6:512–20.
27. Drzewiecki GM, Melbin J, Noordegraaf A. Arterial tonometry: review and analysis. J Biomech 1983;16:141–53.
28. Kelly R, Hayward C, Ganis J, Daley J, Avolio A, O'Rourke M. Noninvasive registration of the arterial pressure waveform using high-fidelity applanation tonometry. J Vasc Med Biol 1989;1:142–9.
29. Kelly R, Karamanoglu M, Gibbs H, O'Rourke M. Noninvasive carotid pressure wave registration as an indicator of ascending aortic pressure. J Vasc Med Biol 1989;1:241–7.
30. Kelly R, Fitchett D. The non-invasive determination of aortic input impedance and external left ventricular power output. A validation and repeatability study of a new technique. J Am Coll Cardiol 1992;20:952–63.
31. London G, Guerin A, Pannier B, Marchais S, Benetos A, Safar M. Increased systolic pressure in chronic uremia: role of arterial wave reflections. Hypertension 1992;20:10–9.
32. Hamilton WF, Dow P. An experimental study of the standing waves in the pulse propagated through the aorta. Am J Physiol 1939;125:48–59.
33. Schnabel TG Jr, Fitzpatrick HF, Peterson LH, Rashkind WJ, Talley D, Raphael RL. A technic of vascular catheterization with small plastic catheters. Its utilization to measure the arterial pulse wave velocity in man. Circulation 1952;5:257–62.
34. Kelly R, Daley J, Avolio A, O'Rourke M. Arterial dilation and reduced wave reflection. Benefit of dilevalol in hypertension. Hypertension 1989; 14:14–21.
35. Roman MJ, Pini R, Pickering TG, Devereux RB. Comparison of noninvasive measures of arterial compliance in normotensive and hypertensive adults. J Hypertens 1992;10 Suppl 6:s115–8.
36. Peterson LN, Jensen RE, Parnell R. Mechanical properties of arteries in vivo. Circ Res 1960;8:622–39.
37. O'Rourke MF. Arterial stiffness, systolic blood pressure and logical treatment of arterial hypertension. Hypertension 1990;15:339–47.
38. Kawasaki T, Sasayama S, Yagi SI, Asakawa T, Hirai T. Non-invasive assessment of the age related changes in stiffness of major branches of the human arteries. Cardiovasc Res 1987;21:678–87.
39. Hirai T, Sasayama S, Kawasaky T, Yagi SI. Stiffness of systemic arteries in patients with myocardial infarction. A noninvasive method to predict severity of coronary atherosclerosis. Circulation 1989;80:78–86.
40. Crunch[4] Statistical Package, User's Manual: Statistics. Oakland, CA: Crunch Software Corporation, 1992;2:362–4.
41. Einot I, Gabriel KR. A study of the powers of several methods of multiple comparisons. J Am Stat Assoc 1975;70:574–83.
42. Freis ED, Heath WC, Luchsiger P, Snell RE. Changes in the carotid pulse which occur with age and hypertension. Am Heart J 1966;71:757–65.
43. Fujii M, Yaginuma T, Noda T, et al. Noninvasive detection for wave reflection in the arterial system, by using carotid pulse wave, and its clinical application. J Jpn Coll Angiogr 1989;29:545–51.
44. Avolio A. Ageing and wave reflection. J Hypertens 1992;10 Suppl 6:S-83–6.
45. London GM, Guerin AP, Pannier BM, Marchais SJ, Metivier F. Body height as a determinant of carotid pulse contour in humans. J Hypertens 1992;10 Suppl 6:S-93–5.
46. Grossman W, Jones D, Mc Laurin LP. Wall stress and patterns of hypertrophy in the human left ventricle. J Clin Invest 1975;56:56–64.
47. Laskey WA, Reichek N, St John Sutton M, Untereker WJ, Hirshfeld JW Jr. Myocardial oxygen consumption in left ventricular hypertrophy and its relation to left ventricular mechanics. Am J Cardiol 1983;52:852–8.
48. Cooper G IV. Cardiocyte adaptation to chronically altered load. Annu Rev Physiol 1987;49:501–18.
49. Mann DL, Kent RL, Cooper G IV. Load regulation of the properties of adult feline cardiocytes: growth induction by cellular deformation. Circ Res 1989;64:1079–90.
50. Darne B, Girerd X, Safar M, Cambien F, Guize L. Pulsatile versus steady component of blood pressure: a cross-sectional analysis and a prospective analysis on cardiovascular mortality. Hypertension 1989;13:392–400.
51. Safar ME, Toto-Moukouo JJ, Bouthier JA, et al. Arterial dynamics, cardiac hypertrophy and antihypertensive treatment. Circulation 1987;75 Suppl I:I-156–61.
52. Pannier B, Brunel P, El Aroussy W, Lacolley P, Safar ME. Pulse pressure and echocardiographic findings in essential hypertension. J Hypertens 1989;7:127–32.
53. Wolinsky H. Long-term effects of hypertension on the rat aortic wall and their relation to concurrent aging changes. Morphological and chemical studies. Circ Res 1972;30:301–9.